Inorganic Chemistry

Article

pubs.acs.org/IC

Heteroleptic Metallosupramolecular Racks, Rectangles, and Trigonal Prisms: Stoichiometry-Controlled Reversible Interconversion

Subhadip Neogi,*[,†] Yvonne Lorenz,[‡] Marianne Engeser,[‡] Debabrata Samanta,[†] and Michael Schmittel*[,†]

[†]Center of Micro and Nanochemistry and Engineering, Organische Chemie I, Universität Siegen, Adolf-Reichwein-Strasse 2, D-57068 Siegen, Germany

[‡]Kekulé-Institut für Organische Chemie und Biochemie, Universität Bonn, Gerhard-Domagk-Strasse 1, 53121 Bonn, Germany

Supporting Information

ABSTRACT: A simple approach toward preparation of heteroleptic two-dimensional (2D) rectangles and three-dimensional (3D) triangular prisms is described utilizing the HETPYP (HETeroleptic PYridyl and Phenanthroline metal complexes) concept. By mixing metal-loaded linear bisphenanthrolines of varying lengths with diverse (multi)-pyridine (py) ligands in a proper ratio, six different self-assembled architectures arise cleanly and spontaneously in the absence of any template. They are characterized by ^{1}H and DOSY NMR, ESI-FT-ICR mass spectrometry as well as by Job plots and UV−vis titrations. Density functional theory (DFT) computations provide information about each structure. A stoichiometry-controlled supramolecule-to-supramolecule interconversion based on the relative amounts of metal bisphenanthroline and bipyridine forces the rectangular assembly to reorganize to a rack architecture and back to the rectangle, as clearly supported by variable temperature and DOSY NMR as well as dynamic light scattering data. The highly dynamic nature of the assemblies represents a promising starting point for constitutional dynamic materials.

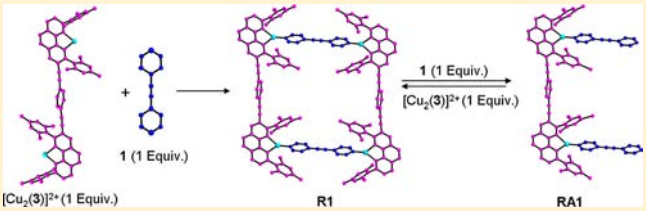

INTRODUCTION

With a large variety of successful strategies being readily available to prepare two-dimensional (2D)[1] and three-dimensional (3D)[2] supramolecular architectures, attention has recently turned to functional dynamic structures that are able to modulate their properties by directed compositional, constitutional, and conformational changes. Detailed mechanistic studies are thus important for understanding responsive self-assemblies and their use in potential applications.[3] So far, the majority of work has focused on hydrogen-bond driven[4] assemblies and constitutionally dynamic[5] assemblies, but rarely on coordination-driven[6] self-assembly. As a notable example for the latter category, Stang and co-workers recently described the transformation of fused metallacyclic polygons through stoichiometric control of multicomponent mixtures and the supramolecular fusion of two 2-component homoleptic architectures into a 3-component heteroleptic system by virtue of charge separation.[7] Lately, Schmittel and co-workers even fabricated a 5-component scalene triangle by the 2-methylpyridine-catalyzed supramolecular fusion of a 3-component rectangle and a 2-component equilateral triangle.[8]

Herein, we will present a three-component self-assembly toward the template-free formation of 2D and 3D supramolecules, such as fully dynamic racks, rectangles, and prisms, and their responsiveness to a variation of the components' ratio. Despite the topological simplicity of our target structures, their multicomponent preparation requires perfect heteroleptic control. For example, synthesis of supramolecular rectangles is often hampered by competitive formation of homoleptic squares. Fortunately, there are various protocols to solve the problem, with complexity rising significantly upon increasing the number of components. By attaching a platinum-based molecular clip with two parallel donor sites to linear ditopic ligands, Stang and others self-assembled molecular rectangles.[1a,6e] Using orthogonal binding motifs, that is, by connecting a bis-chelating dianion to the equatorial sites of two *fac*-$(CO)_3$Re cores and a ditopic nitrogen-donor ligand, Lu and co-workers prepared rectangles in high yield.[1j] Likewise, prisms may be prepared. The simplest way of designing a trigonal prism, is to use a two-component assembly. Based on the directional bonding approach, Stang, and co-workers have designed trigonal prisms using a 0° Pt-based molecular clip and planar tripodal linkers by a 3 + 2 self-assembly reaction.[2a] More control is required in the three-component protocol, as reported by Fujita and co-workers. A combination of an end-capped acceptor, a tritopic planar donor, and a bidentate linear donor in a 6:2:3 molar ratio furnished the desired prism.[2c] Recently, Lusby even reported on a kinetically controlled four-component synthetic approach to trigonal prisms.[2e]

As already stated above, structural transformations and interconversions[9] of discrete self-assembled metallosupramolecules in solution have rarely been studied. Such protocols essentially require, in contrast to traditional design principles, to instate additionally an unique bidirectional sensitivity toward external inputs. Herein, we will describe a reversible supra-

Received: February 7, 2013
Published: June 5, 2013

dx.doi.org/10.1021/ic400328d | *Inorg. Chem.* 2013, 52, 6975−6984

Scheme 1. Schematic Illustration of Known Heteroleptic Complexation Motifs

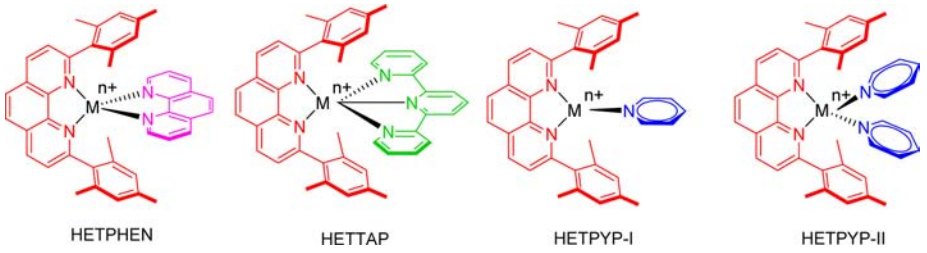

Scheme 2. Ligands Used in the Present Study (with Atom Numbering Scheme)

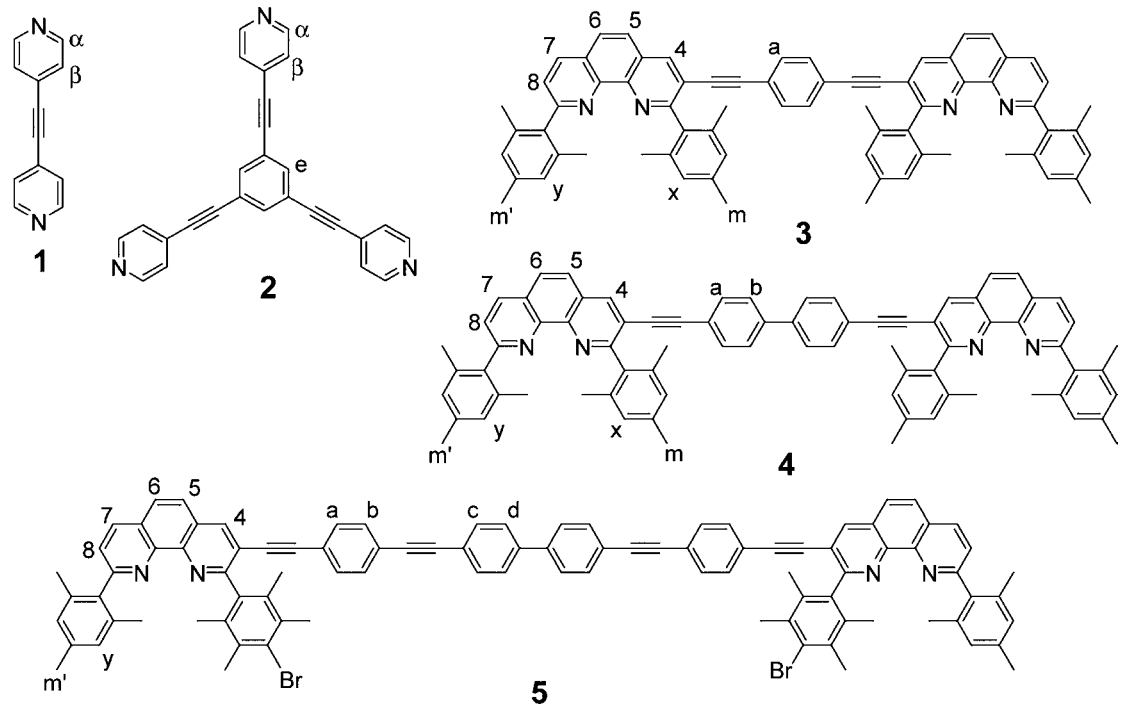

molecule-to-supramolecule structural alteration upon varying the ratio of components. The self-assembly will be based on mixed phenanthroline pyridine copper(I) complexes.

The sterically shielded 2,9-diarylphenanthroline ($phenAr_2$) has proven itself as a versatile capping unit for the quantitative formation of a variety of nanosized heteroleptic supramolecular assemblies either via the HETPHEN (HETeroleptic bis-PHENanthroline complexes)[10] or the HETTAP (HETeroleptic Terpyridine And Phenanthroline complexes)[11] approach (Scheme 1). However, exchange of one or several bi- or tridentate ligands at dynamically binding metal ions operates at the cost of slow kinetics. HETPHEN and HETTAP coordination scenario are thus not ideal for establishing facile and possibly rapid interconversion of supramolecules. As a promising alternative, we recently developed the HETPYP (HETeroleptic PYridine and Phenanthroline metal complexes)[12] concept (Scheme 1) and prepared a series of discrete three-component architectures in solution and the solid state.[12c] The principal structural and bonding features are as follows: (i) the combination of the sterically encumbered phenanthroline ligand **L** and a metal ion M^{n+} will generate a capped $[M(\mathbf{L})]^{n+}$ unit, in which the metal ion is still accessible for the "slim" pyridine ligand; (ii) the $\pi-\pi$ interaction between the 2,9-diaryl substituents of **L** and the pyridine ligand stabilizes the heteroleptic combination; (iii) the geometric arrangement encoded in individual subunits and their stoichiometric ratio opens up a general platform to construct either trigonal (HETPYP-I) or tetragonal (HETPYP-II) coordination scenarios[13] at the metal center (Scheme 1).

Using the fact that each capped copper(I) center can effectively accommodate one pyridine ligand in the HETPYP-I complexation scenario, we report herein the synthesis of various discrete heteroleptic two- and three-dimensional architectures by mixing preorganized linear metalated bis-phenanthroline building blocks with oligopyridine ligands (Scheme 2) in a proper ratio. Furthermore, we demonstrate a reversible structural changeover between discrete rectangle and rack assemblies, simply by tuning the pyridine/$[Cu_2(\mathbf{L})]^{2+}$ ratio (**L** = **3**, **4**) (Scheme 2). Such receptiveness should open the option to switch emergent properties of multicomponent systems in response to the deliberate addition and removal of components, via shuffling. So far, manifestations of rapid additive-triggered supramolecule-to-supramolecule (inter)-conversions in metallosupramolecular chemistry are rare.[7,8,9a−c]

RESULTS AND DISCUSSION

Pyridylethynyl units were incorporated into **1** and **2**, via routine Sonogashira coupling,[14] to provide conformational flexibility for coordination to the capped copper(I) center. The bisphenanthrolines **3** and **4** controlling the HETPYP-I coordination were

dx.doi.org/10.1021/ic400328d | Inorg. Chem. 2013, 52, 6975−6984

synthesized according to published procedures[15] while ligand **5** was readily accessible via a Sonogashira cross-coupling reaction of 2-(4-bromo-2,3,5,6-tetramethylphenyl)-3-(4-iodophenylethynyl)-9-mesityl-[1,10]-phenanthroline and 4,4′-diethynylbiphenyl (Scheme S1, Supporting Information).

X-ray Structure of Ligand 4. In addition to the solution state characterization,[15] it was also possible to establish the structure of **4** (Scheme 2) by single crystal X-ray analysis. Figure 1 shows that the structure is centrosymmetric with an inversion center at the midpoint of the biphenyl spacer unit. Thus, the molecule displays a transoid conformation. The crystal packing shows a number of weak intermolecular $\pi-\pi$ and C−H···π interactions.

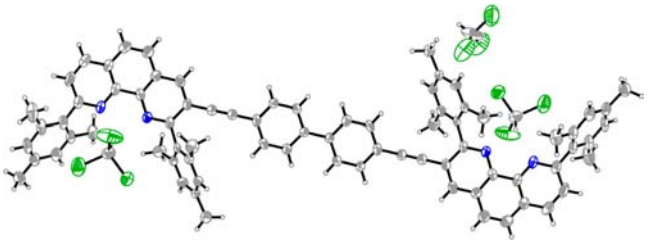

Figure 1. Solid state structure of **4** with displacement ellipsoids at the 50% probability level.

Synthesis of Supramolecular Rectangles R1−R3. Clean formation of **R1**, as concluded from NMR, VT-NMR (vide infra), DOSY, MS and DLS data, is observed upon mixing the copper bisphenanthroline $[Cu_2(\mathbf{3})]^{2+}$ (Cu^+:**3** = 2:1) and ligand **1** in a 1:1 ratio in dichloromethane. The ^{1}H NMR spectrum reveals only one set of sharp signals, where coordination of the positively charged metal center results in typical downfield shifts for all protons at the phenanthroline core (Table 1). In contrast, the chemical shifts of the pyridine α-H are drastically shifted upfield from 8.63 to 6.82 ppm while pyridine β-H experience a shift from 7.42 to 7.22 ppm (Figure 2). The upfield shifts suggest that each pyridine ring of **1** is located within the cavity of the $[Cu_2(\mathbf{3})]^{+2}$ unit so that protons α-H experience strong shielding effects from the mesityl groups of **3**. This observation is in line with our previous findings and implies a tricoordination at each copper(I) center.[12c] Peak assignments are further substantiated by COSY experiments. In accordance with ^{1}H NMR results, analysis of the ^{13}C NMR spectrum of the reaction mixture reveals only 25 aromatic, 3 acetylenic, and 4 aliphatic peaks (Figure S5, Supporting Information), corroborating a time-averaged D_{2h} symmetric structure.

ESI-FT-ICR mass spectra obtained using extremely soft ESI conditions[16] furnished added support for **R1** because signals are seen for the doubly and triply charged aggregate with correct isotope patterns and exact masses (Figure 3). The most abundant fragment, formed during the ESI process from **R1** in acetone, contains a $[Cu_2(\mathbf{3})]^{2+}$ core with one or two additionally coordinated molecules **1**. Thus, the gas-phase data fully confirm HETPYP-I complexation in **R1**. While the strongly bound $[Cu_2(\mathbf{3})]^{2+}$-entities mostly stay intact in the gas phase, the rather weakly binding pyridine ligands easily dissociate in presence of excess energy. The latter property is imperative for the use of this complex motif in the construction of a highly dynamic supramolecular structure.[12] Further evidence toward the formation of **R1** was obtained from the method of continuous variation (Job plot) in UV−vis titrations, indicating (Figure 3a) a perfect 1:1 stoichiometry of $[Cu_2(\mathbf{3})]^{2+}$ and ligand **1** at 25 °C.

More information on the structure of the metallosupramolecular rectangle was obtained from ^{1}H NMR DOSY (diffusion-ordered spectroscopy) and DLS (dynamic light scattering) experiments, carried out at 25 °C in dichloromethane. A single diffusion coefficient in the DOSY NMR (Figure 3b) points toward sole formation of **R1** with $D = 3.8 \times 10^{-10}$ m^2 s^{-1}. The experimental hydrodynamic diameter derived therefrom[17] matches well with the value obtained from the DLS measurement and the energy minimized structure[18] (Table 2 and Table S2, Supporting Information), indicating that the solution assembly of **R1** is in good agreement with its theoretically predicted structure.

Since suitable single crystals for X-ray diffraction measurements could not be obtained, DFT computations were used to gain further insight into the structural characteristics of **R1**. The energy-minimized structure is calculated with Gaussian03[19] using the B3LYP/6-31G(d) exchange correlation functional[20]

Table 1. Characteristic ^{1}H NMR (400 MHz, 25 °C) with Selected Chemical Shifts (in ppm) of the Ligands (see Scheme 2) and Complexes

	phenanthroline protons				pyridine protons			
ligands/Complexes[a]	4	7	5,6	8	H_α	$\Delta\delta$ (H_α)[c]	H_β	$\Delta\delta$ (H_β)[c]
1					8.63		7.42	
2					8.62		7.42	
3	8.49	8.33	7.86−7.93	7.57				
4	8.51	8.33	7.87−7.93	7.57				
5[b]	8.47	8.29	7.85−7.90	7.58				
R1	8.83	8.71	8.16−8.20	7.94	6.82	1.81	7.22	0.20
R2	8.83	8.71	8.16−8.20	7.94	6.84	1.79	7.22	0.20
R3	8.85	8.73	8.18−8.22	7.97	7.03	1.60	7.27	0.15
P1	8.82	8.70	8.16−8.20	7.94	6.88	1.74	7.20	0.22
P2	8.83	8.71	8.16−8.20	7.94	6.86	1.76	7.20	0.22
P3	8.84	8.72	8.16−8.20	7.96	6.93	1.69	7.23	0.19
RA1	8.84	8.71	8.16−8.20	7.94	7.66	0.97	7.31	0.11
RA2	8.85	8.72	8.17−8.21	7.94	7.66	0.97	7.31	0.11

[a]Recorded in CD_2Cl_2. [b]Recorded in $CDCl_3$. [c]^{1}H NMR shift difference for H_α or H_β between the uncoordinated pyridine ligand and its resultant complexes.

dx.doi.org/10.1021/ic400328d | Inorg. Chem. 2013, 52, 6975−6984

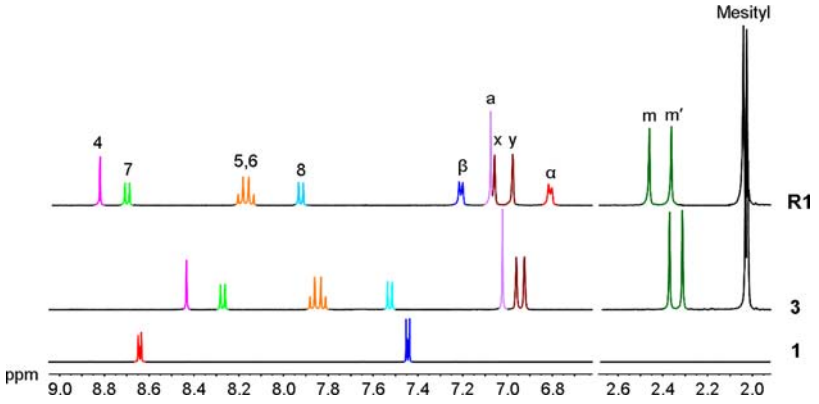

Figure 2. ^{1}H NMR spectra (partial, 400 MHz, 25 °C) of **1**, **3** and complex **R1** (pyridine α and β protons are shown in red and blue color, respectively).

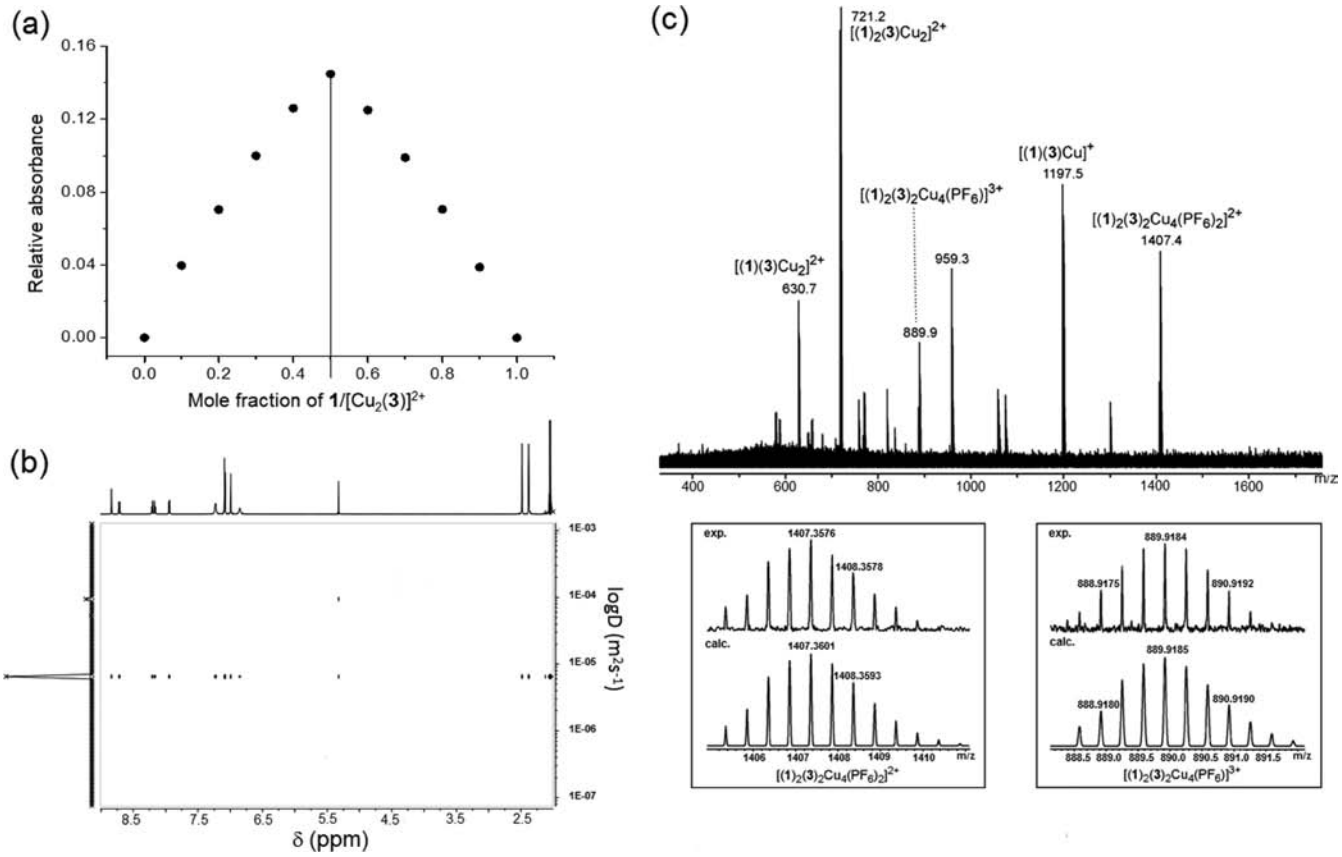

Figure 3. Data on **R1**: (a) Job plot from a UV−vis titration showing 1:1 stoichiometry for 1/[Cu_2(3)]$^{2+}$, (b) ^{1}H DOSY spectrum, and (c) ESI-FT-ICR mass spectrum with isotope distribution patterns for the doubly and triply charged aggregates.

in conjunction with LANL2DZ effective core potentials[21] for copper, nicely illustrating the rectangular arrangement of **R1** (Figure 4).

To further extend the scope of the HETPYP-I approach and evaluate the size limit of the self-assembled rectangles attainable, we employed ligands **4** and **5** with 31 Å and 47 Å length, respectively, in combination with **1** and copper(I) ion. Analogously as for **R1**, the reaction of the individually capped copper complexes [Cu_2(**L**)]$^{2+}$ (**L** = **4**, **5**) with ligand **1** (1:1 ratio) yielded cleanly the supramolecular rectangles **R2** and **R3**. The spectroscopic characterization and evaluation of purity was performed as for **R1** and shall not be presented in details here but in the Supporting Information. For the other rectangles **R2**, **R3** (Figure 4), equally DFT computations provided energy minimized structures that are in agreement with DLS and DOSY results. The energy minimized structures in **R1**−**R3** show planes of bisphenanthroline and **1** to be perpendicular thus increasing the π-stacking interactions between mesityl and pyridine rings that appear to stabilize the overall structure.

Synthesis of Supramolecular Triangular Prisms P1−P3. The successful formation of discrete trigonal prismatic cages **P1**−**P3** from the tritopic connector **2** (Scheme 2) and various capped copper complexes [Cu_2(**L**)]$^{2+}$ (**L** = **3**, **4**, **5**) proceeded without template assistance. As a representative example for all the cases studied so far, we report in detail on the formation of **P1** in dichloromethane. Because oligopyr-

dx.doi.org/10.1021/ic400328d | Inorg. Chem. 2013, 52, 6975−6984

Table 2. Diffusion Coefficients, Hydrodynamic Diameters, and Modeled Diameters of All the Complexes

Complex	D [10^{-10} m^2s^{-1}][a,b]	d_H (DOSY) [nm][a,c]	d_H (DLS) [nm][a]	d_{av} (calcd) [nm][d] (Model)
R1	3.8	2.72	2.81	2.82
RA1	4.5	2.30	2.48	
R2	3.4	3.04	3.13	3.09
RA2	4.0	2.58	2.71	
R3	2.8	3.68	3.77	3.91
P1	3.6	2.86	2.99	3.00
P2	3.2	3.22	3.38	3.30
P3	2.7	3.82	3.98	4.06

[a]All measurements done at 25 °C in dichloromethane. [b]Diffusion coefficient obtained from the 2D DOSY NMR experiments. [c]Hydrodynamic radii calculated via the Stokes−Einstein equation $D = k_BT/6\pi\eta r_H$ (k_B, Boltzmann constant; T, absolute temperature; η, viscosity of CH_2Cl_2 at 298 K). [d]Average diameter $d_{av} = (d_v + d_h + d_d)/3$ (see Table S2, Supporting Information).

idines typically form oligomeric complexes in the presence of many metal ions[22] it is advisable to avoid formation of any unwanted kinetically locked complex right at the onset by combining all components sequentially. Accordingly, **3** is first fed with 2 equiv of Cu^+ in dichloromethane-d_2 to form the capped and coordinatively unsaturated complex $[Cu_2(\mathbf{3})]^{2+}$ as a clear pale yellow solution. After mixing ligand **2** with $[Cu_2(\mathbf{3})]^{2+}$ in a 2:3 stoichiometric ratio, the color of the sonicated solution intensifies to deep yellow. A combination of ^{1}H NMR, ^{1}H-^{1}H COSY, ^{13}C NMR, and DOSY NMR spectroscopy verifies the clean formation of **P1**. The ^{1}H NMR spectrum of the mixture reveals only one set of sharp signals, with all phenanthroline protons being shifted upfield because of metal complexation. The most diagnostic upfield shift is observed for the pyridine α-H ($\Delta\delta$ = 1.74 ppm), while pyridine β-H ($\Delta\delta$ = 0.22 ppm) are less shifted to upfield (Table 1). This observation is in line with the attachment of one pyridine ring to each coordinatively unsaturated copper(I) center of the $[Cu_2(\mathbf{3})]^{2+}$ unit. The proton corresponding to the central benzene ring of **2** experiences a slight downfield shift (Figure 5) upon complexation ($\Delta\delta$ = 0.12 ppm).

The complex is further studied by ^{1}H DOSY spectroscopy (Figure S25, Supporting Information), indicating the formation of a single product. The ^{13}C NMR spectrum of the solution reveals 27 aromatic, 4 acetylenic, and 4 aliphatic peaks (Figure S27, Supporting Information) suggesting the formation of a time averaged D_{3h} symmetric structure. The Job plot shows an ideal 2:3 stoichiometry (Figure 6a) of ligand **2** and $[Cu_2(\mathbf{3})]^{2+}$. ESI FT-ICR mass spectrometry of the yellow solution of **P1** shows (Figure 6c) signals for the molecular species $[Cu_6(\mathbf{3})_3(\mathbf{2})_2(PF_6)_3]^{3+}$, $[Cu_6(\mathbf{3})_3(\mathbf{2})_2(PF_6)_2]^{4+}$, and $[Cu_6(\mathbf{3})_3(\mathbf{2})_2(PF_6)]^{5+}$ with correct isotope patterns and exact mass in addition to the expected fragments, in which again the $[Cu_2(\mathbf{3})]^{2+}$ building blocks remain intact.

A battery of experimental evidence thus asserts that the rare trigonal coordination motif of copper(I) can be realized in presence of phenanthroline **3** and the weakly binding pyridine **2**, leading to exclusive formation of **P1** without a template or additional directing factors. The latter bonding, as extensively described in our earlier work,[12c] is further characterized by strong $\pi-\pi$ stacking between the pyridine ring and mesityl groups of bisphenanthroline **3**.

Analogously, following a 3:2 stoichiometric ratio of the respective capped pillar complex $[Cu_2(\mathbf{L})]^{2+}$ (**L** = **4**, **5**) and ligand **2**, the heteroleptic prisms **P2** and **P3** were obtained exclusively, as evident from spectroscopic data (see full spectroscopic characterization in Supporting Information) and elemental analysis.

Suitable X-ray-quality crystals were not obtained for any of the prisms **P1**−**P3**. Theoretical computation using Gaussian03 at the B3LYP/6-31G (d) level (for **P1** and **P2**) were thus performed (Table S3, Supporting Information) to obtain some information about their structure and differently sized voids, because the supramolecular prisms may become useful in host−guest chemistry and as microreactors. Taking the Cu−Cu distance as a measure, the model structure of **P1** features a well-defined trigonal prism with respective height, width, and diagonal of 1.8, 1.7, and 2.5 nm (Figure 7). The roof is covered by one *tris*-pyridine ligand **2** while each corner is defined by a three-coordinate Cu^+ ion. The computation of **P2** shows a similar trigonal structure with larger dimensions than in **P1**. The ball-and-stick model for **P3**, computed using the semiempirical method PM6 divulges the largest dimensions among the three prism assemblies: ∼3.5 nm (height), ∼1.7 nm (width), and ∼4.0 nm (Cu−Cu diagonal). For all the nanoprisms the pyridine rings of ligand **2** adopt a parallel orientation with respect to the mesityl's aromatic plane of **L** (**L**= **3**, **4**, **5**) to maximize $\pi-\pi$ stacking, but as a result the overlap with the central benzene spacer is reduced. The

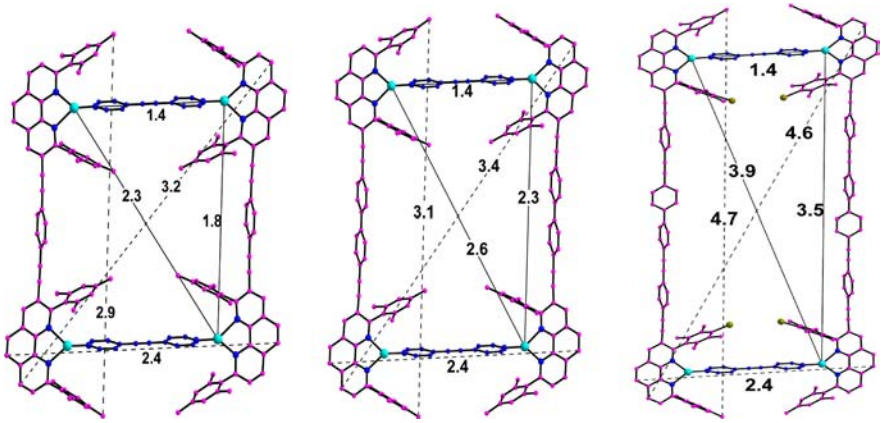

Figure 4. DFT calculated structures of **R1**, **R2**, and **R3** (from left to right) in ball-and-stick representations. Cu−Cu distances (solid lines) and measures between two furthest atoms (dotted lines; vertical, horizontal, and diagonal) are depicted (in nm). Hydrogen atoms are omitted for clarity.

dx.doi.org/10.1021/ic400328d | *Inorg. Chem.* 2013, 52, 6975−6984

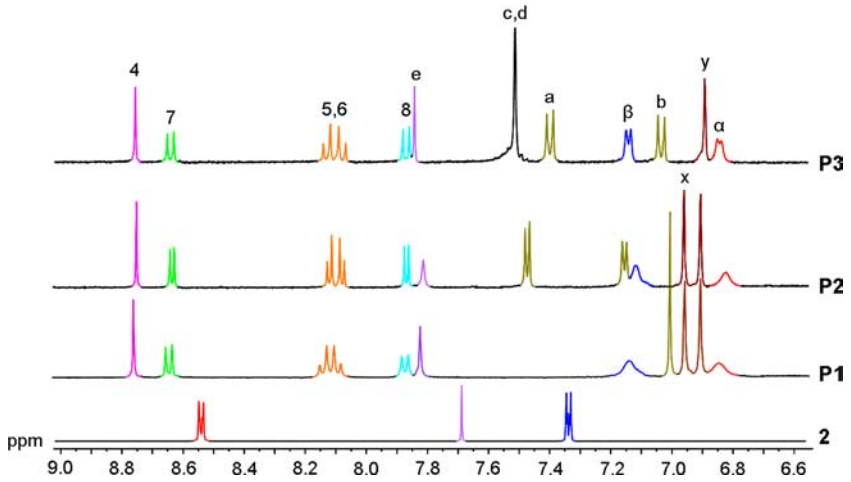

Figure 5. Partial ^{1}H NMR spectra (400 MHz, 25 °C, CD_2Cl_2) of **2** and each prism assembly. Pyridine α and β protons are shown in red and blue color, respectively.

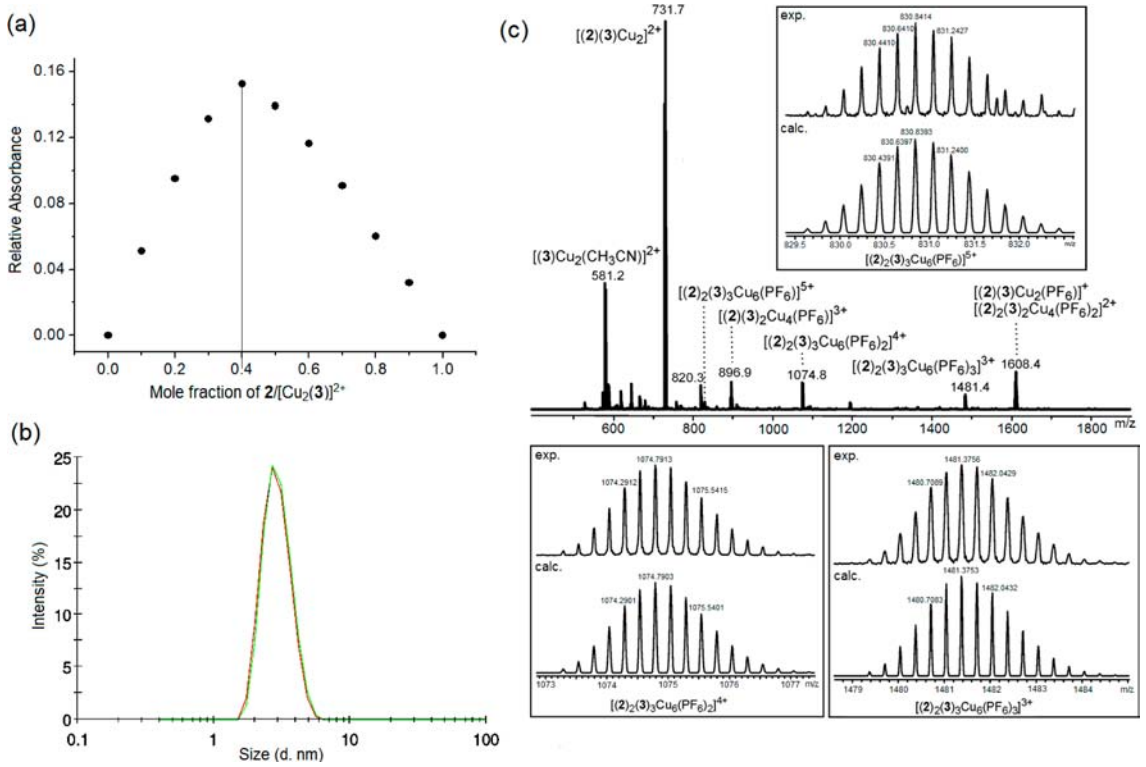

Figure 6. Data for supramolecular prism **P1**: (a) Job plot, (b) dynamic light scattering data, and (c) ESI FT-ICR mass spectrum including the experimental and calculated isotopic distributions of 3^+, 4^+, and 5^+ charged species.

augmented geometric strain for **P1**−**P3**, as a consequence to maximize π−π stacking, is also reflected by a pronounced bending in bisphenanthroline pillar ligands in the energy minimized structures. The hydrodynamic diameter of each prism assembly (Table 2), as determined from DOSY NMR,[17] shows an excellent agreement with the data obtained from dynamic light scattering experiments and the average size (d_{av})[18c] as derived from computed vertical, horizontal, and diagonal distances between the two furthest separated atoms in the respective prisms (Figure 7 and Supporting Information, Table S2).

The structural closeness of all assemblies is best recognized from the NMR shift differences $\Delta\delta(H_\alpha)$ and $\Delta\delta(H_\beta)$ at the pyridine ring (Table 1) that witness sensibly the different spatial arrangement of the pyridine ring in the respective assembly as compared to the situation in the free ligand. The numbers indicate that for both individual series of rectangles or prisms, the $\Delta\delta$ values are remarkably constant.

Stoichiometry-Induced Interconversion from Rectangle to Rack Assembly. An instant reorganization of **R1** was detected in a ^{1}H NMR titration experiment (Figure 8), in which a diagnostic downfield shift of the α pyridine protons from 6.82 to 6.96 ppm is witnessed at little excess of **1** (total 1.2 equiv.), while the pyridine β protons experience a slight shift from 7.22 to 7.27 ppm. Further addition of **1** (total 1.5 equiv.) to the solution promotes an extra downfield shift of pyridine α and β protons, attesting a dynamic behavior of the assembly. At 2.0 equiv of **1** (**1**/$[Cu_2(3)]^{2+}$= 2: 1), the pyridine α and β

dx.doi.org/10.1021/ic400328d | Inorg. Chem. 2013, 52, 6975−6984

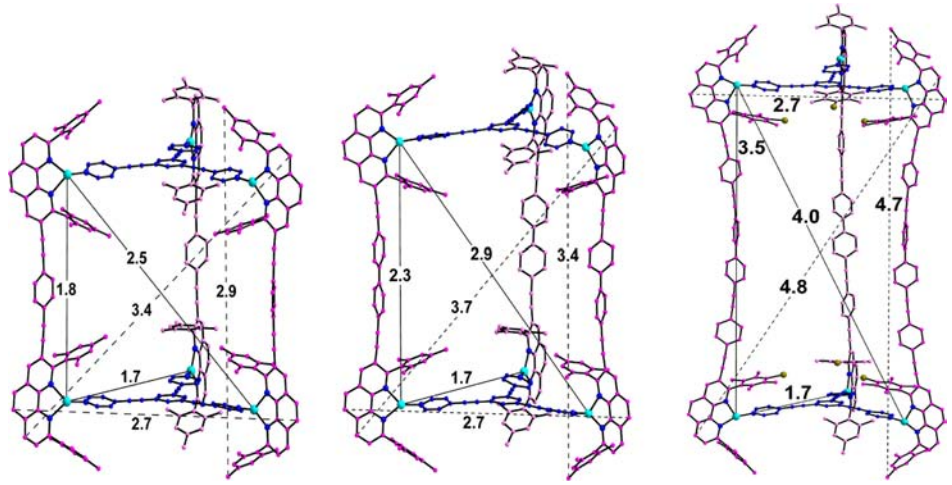

Figure 7. Structural features of **P1**, **P2**, and **P3** in ball and stick representations, derived from the respective energy minimized structures. Cu−Cu distances (in solid lines) and measures between two furthest atoms (dotted lines; vertical, horizontal, and diagonal) are considered (in nm). Hydrogen atoms are omitted for clarity.

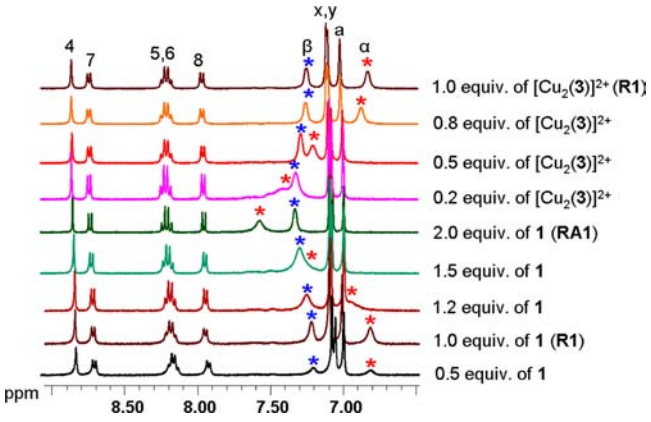

Figure 8. ^{1}H NMR titration (partial spectrum, 400 MHz, RT) leading to stepwise developmentof **R1** and **RA1**, starting from $[Cu_2(\mathbf{3})]^{2+}$ with varying ratios of **1**, plus back-titration of **RA1** by addition of $[Cu_2(\mathbf{3})]^{2+}$ to reform **R1**.

protons appear as two separate broad singlets at 7.66 and 7.31 ppm, respectively (Table 1), suggesting the formation of a different species. Clearly, both α and β pyridine protons now experience less shielding by the mesityl group of **3**. Absence of any precipitation additionally confirms that no homoleptic pyridine/oligomer complexes form in between the transformations. However, further addition of **1** (3.0 equiv.) causes immediate precipitation consistent with oligomer formation, precluding supplementary NMR measurement.

Although the ^{1}H NMR DOSY of the newly formed assembly at **1**/$[Cu_2(\mathbf{3})]^{2+}$ = 2:1 advocates a single trace (Figure S45, Supporting Information) with no peaks found for free pyridine protons, its diffusion coefficient was found to be larger than that of **R1** (Table 2). Furthermore, a DLS study on rectangle **R1** and the new assembly reveals a different monomodal size distribution for both assemblies (Figure 9) with hydrodynamic diameters d = 2.48 nm (for the unknown assembly) and 2.81 nm (for **R1**). Both diameters match with the size determination from DOSY NMR[18] (Table 2) thus suggesting that the new HETPYP assembly at a ratio of $[Cu_2(\mathbf{3})]^{2+}$/ **1** = 1: 2 is smaller than **R1**.

Because ESI-FT-ICR mass spectra, even under very soft ionization condition, do not allow us to establish unambiguously the structure of the unknown assembly, we have to argue solely on the basis of solution data. In principle, the **R1** assembly with its coordinatively unsaturated Cu^+ ion can expand its coordination number from three to four (HETPYP-I→HETPYP-II)[12c] in presence of excess of pyridine ligand (**1**/$[Cu_2(\mathbf{3})]^{2+}$ = 2:1), leading to either an oligomeric assembly or a discrete prism. However, based on the size data collected from DLS and DOSY experiments, the possibility of a larger architecture can be excluded. Formation of oligomeric assembies has already been ruled out in the preceding section.

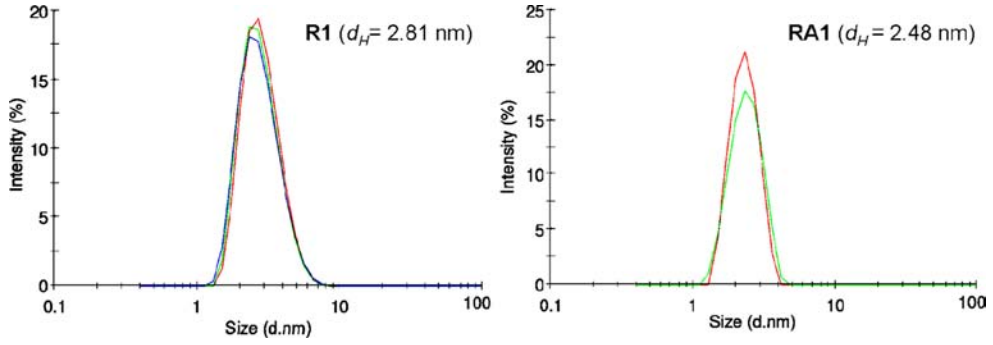

Figure 9. Dynamic light scattering data showing difference in monomodal size distribution curves and hydrodynamic diameters for **R1** and **RA1**. Various colored traces represent individual measurements.

dx.doi.org/10.1021/ic400328d | *Inorg. Chem.* 2013, 52, 6975−6984

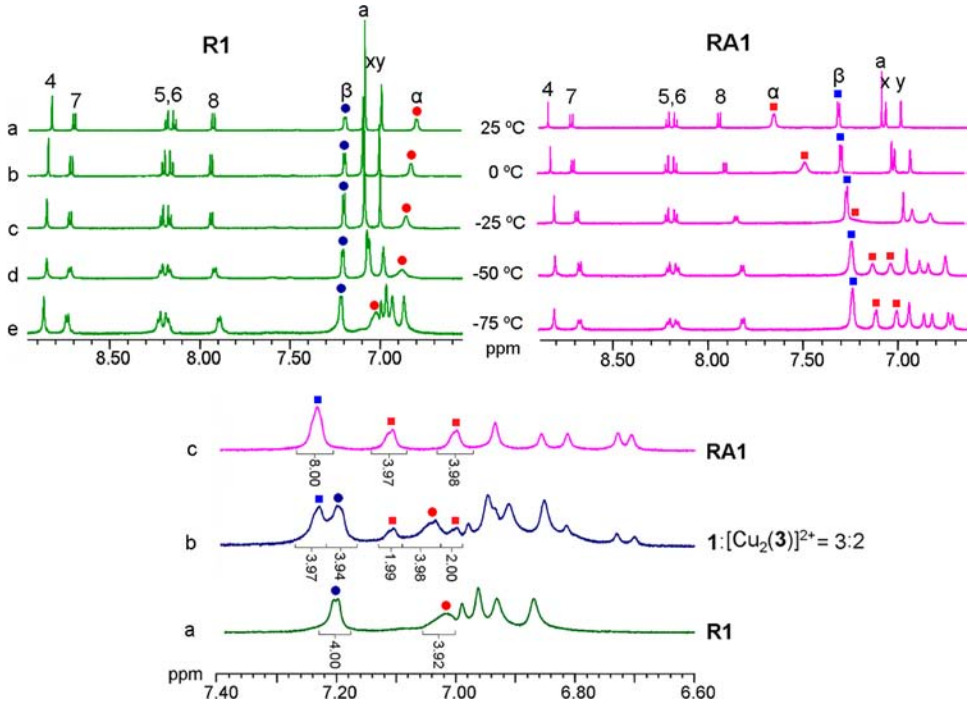

Figure 10. Top: Variable temperature ^{1}H NMR spectra (400 MHz, in CD_2Cl_2) of **1**/$[Cu_2(\mathbf{3})]^{2+}$ = 1:1 (**R1**) and 2:1 (**RA1**). Color code: **R1**, green; RA1, pink; py_α, red; py_β, blue. Bottom: Low temperature (−75 °C) partial ^{1}H NMR spectra of (a) **R1**, (b) the products arising from a mixture of **1**/$[Cu_2(\mathbf{3})]^{2+}$ = 3:2 and (c) **RA1**.

Scheme 3. Cartoon Representation for the Construction of R1 and the Additive Triggered Dynamic Interconversion to Rack Assembly

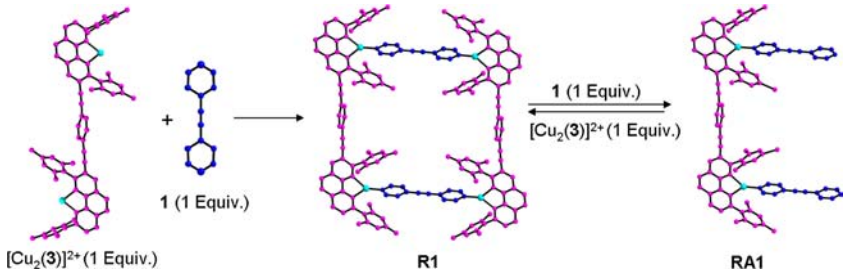

Based on thermochemical reasoning (vide infra), the simplest structure formed from **1**/$[Cu_2(\mathbf{3})]^{2+}$ = 2:1 is the molecular rack **RA1**, where one $[Cu_2(\mathbf{3})]^{2+}$ unit is attached to two ligands **1** at one of their pyridine terminals, while the second pyridine end is left uncoordinated. Such rationale is further substantiated by probing the mixture **1**/$[Cu_2(\mathbf{3})]^{2+}$ at various ratios, that is, 1:1 (= **R1**) and 2:1 (= **RA1**), and different temperatures in ^{1}H NMR (Figure 10, top). The signals of the pyridine α-H of **1** are of particular help, as upon decreasing the temperature, they experience a gradual shift. In contrast, pyridine β-H do not experience any striking shift upon cooling because of their distant position from the mesityl groups.

In **R1**, the pyridine α-H experience a slight downfield shift with decreasing temperature that is obviously the result of a tighter binding due to the positive ($-T\cdot\Delta S$) term. A somewhat larger downfield shift is seen below −50 °C when protons x-H and y-H split because of freezing of the rotation about the mesityl-phenanthroline axis. The above NMR results (Figure 10, top left) thus suggest that assembly **R1** is dynamic at room temperature mostly because of its rotational freedom about the long axis of **1** (intramolecular). Once the temperature reaches −75 °C, a more rigid conformation is attained, in which the α-H experience strong deshielding by the mesityl groups (Scheme 3).

In contrast, the dynamic nature of the rack assembly **RA1** is much more temperature dependent and more complex. At room temperature, both pyridine terminals exhibit time-averaged[12c] proton signals because of rapid exchange of "free" and "bound" pyridine ends (intermolecular) with an NMR shift placed between those of the free ligand **1** and **R1** (Table 1). At −50 °C, the swapping motion starts to freeze and the single resonance for α-H separates into two resonances (Figure 10, top right). Finally, the $[Cu_2(\mathbf{3})]^{2+}$ units and the pyridine terminals display NMR shifts that increasingly indicate formation of a rack architecture (Scheme 3), mainly based on the splitting of the pyridine α-H (as stated above). At −75 °C, even the dynamics about the single Cu—py coordination bond (rotational) freezes, as deduced from the splitting of the mesityl protons. Obviously, intra- and intermolecular dynamics has now come to a halt. With any of the intermolecular exchange being stopped, we can see at −75 °C from the NMR that **R1** is not contaminated with **RA1** and reciprocally **RA1** is not contaminated with **R1** (Figure 10)

dx.doi.org/10.1021/ic400328d | Inorg. Chem. 2013, 52, 6975−6984

Another crucial piece of information arises from the VT-NMR of **1**/$[Cu_2(\mathbf{3})]^{2+}$ = 3:2 which should correspond to a 1:1 mixture of **RA1** and **R1**. Comparing the low temperature ^{1}H NMR with that of clean **RA1** or **R1**, one realizes that at −75 °C two sets of signals emerge that indeed reflect a mixture of **R1**:**RA1** = 1:1 (Figure 10, bottom). Above that temperature, at about −50 °C, **R1** and **RA1** interconvert already as can be derived from a single set of averaged NMR signals (Figure S51, Supporting Information). The VT-NMR data thus support existence of clean **RA1** or **R1** at the corresponding ratios **1**/$[Cu_2(\mathbf{3})]^{2+}$ of 2:1 or 1:1.

Finally, the stoichiometry-induced conversion of **RA1**→ **R1** is demonstrated in a ^{1}H NMR titration experiment at room temperature. The results as summarized in Figure 8 disclose that increasing addition of complex $[Cu(\mathbf{3})]^{2+}$ to the solution of **RA1** causes both the α and the β pyridine protons to shift upfield in a steady manner. Finally, at 1.0 equiv of $[Cu(\mathbf{3})]^{2+}$, the resulting ^{1}H NMR spectrum precisely matches with that for **R1**. This experiment furthermore demonstrates that the transformation is completely reversible. The process of structural alteration from the rectangular assembly to a rack, by changing the stoichiometric ratio of $[Cu(\mathbf{3})]^{2+}$/ **1**, can be viewed as a supramolecular structural transformation, as a function of the component stoichiometry.

The existence of **RA1** with noncoordinating pyridine terminals is unexpected because it violates the maximum site occupancy rule. However, the exclusive formation of **RA1** and its subsequent equilibration behavior is of no surprise in light of thermochemical reasoning, as the construction of a discrete rack is always entropically favored over poly/oligomeric assemblies. Although, formation of a heteroleptic rack has been documented previously using the HETPHEN concept,[10h] to the best of our knowledge, there are no examples in the literature where the interconversion of a heteroleptic rack and rectangle can be controlled by the relative stoichiometry of individual components. Because of the weak Cu(I)−N(Py) binding energy, the aforesaid changeovers in the supramolecular arrangement are facile.

Based on the above protocol, a fully analogous stoichiometry reliant reversible interconversion of **R2** = $[Cu_4(\mathbf{4})_2(\mathbf{1})_2]^{4+}$ → **RA2** = $[Cu_2(\mathbf{4})(\mathbf{1})_2]^{2+}$ is convincingly established by room temperature ^{1}H NMR (Table 1 and Figure S52, Supporting Information), low temperature ^{1}H NMR (Figure S53, Supporting Information), and further supported by DOSY and DLS measurements (Table 2). Hence, the present study demonstrates a reliable approach to *dynamic* HETPYP-I complexation as a useful design principle for stoichiometry-controlled supramolecular transformations. Such dynamic modulation offers immense importance in the field of functional dynamic materials to introduce stimuli-dependent properties, for example through modifying constitution by exchanging and reshuffling components.[9] Unfortunately, no analogous transformation could be studied for either **R3** or the prism assemblies as excess of pyridine ligands led to precipitation of oligomeric complexes.

CONCLUSION

In conclusion, utilizing the HETPYP-I (HETeroleptic PYridyl and Phenanthroline metal complexes) protocol, the above report details a novel design principle to construct a series of metallosupramolecular rectangle and trigonal prism assemblies in quantitative yield and without any template effect. The present synthetic strategy relies on the successful utilization of sterically encumbered bisphenanthroline ligands to set up a cap, from which the rare trigonal $[Cu(phenAr_2)(py)]^+$ coordination motif can be elaborated, using appropriate bi- and tris-pyridyl ligands. An interesting feature of the present study is the stoichiometry-controlled supramolecule-to-supramolecule transformation, based on the relative amounts of oligopyridines. Excess of bipyridine, for example, **1**, forces the rectangle assembly to alter into a rack architecture in solution. Vice versa, the rectangle can again be reinstalled by titrating the rack architecture $[Cu_2(\mathbf{1})_2(\mathbf{L})]^{2+}$ with $[Cu_2(\mathbf{L})]^{2+}$ (**L** = **3**, **4**). The observed rapid interconversion between the two structures, well supported by variable temperature ^{1}H NMR, arises from the intrinsic dynamic nature of these assemblies owing to the labile d^{10} Cu(I)−N(Py) bond. Although, the formation of rack assemblies violates the maximum site occupancy rule, its formation and subsequent equilibration behavior is of no surprise in light of thermochemical reasoning. Given the great interest in reversible structure alterations in supramolecular assemblies, our study provides a new systematic to modify constitution by exchanging and reshuffling ligand components.

ASSOCIATED CONTENT

Supporting Information

X-ray crystallographic data for **4** in CIF format. Experimental details of synthesis, characterization for ligand **5** and all the complexes, NMR spectra, DLS, FT-IR, and mass spectrometric data, views of the single crystal X-ray structure, coordinates from the computation. This material is available free of charge via the Internet at http://pubs.acs.org.

AUTHOR INFORMATION

Corresponding Author

*E-mail: neogi@chemie.uni-siegen.de (S.N.), schmittel@chemie.uni-siegen.de (M.S.).

Notes

The authors declare no competing financial interest.

ACKNOWLEDGMENTS

We are indebted to the DFG for continued support and to the Alexander von Humboldt Foundation for a stipend to S.N. We thank Dr. J. W. Bats (Frankfurt) for measuring the X-ray data of **4** and M. L. Saha for help with the FT-IR measurements.

REFERENCES

(1) (a) Kuehl, C. J.; Huang, S. D.; Stang, P. J. *J. Am. Chem. Soc.* **2001**, *123*, 9634. (b) Papaefstathiou, G. S.; Zhong, Z.; Geng, L.; MacGillivray, L. R. *J. Am. Chem. Soc.* **2004**, *126*, 9158. (c) Yue, N. L. S.; Jennings, M. C.; Puddephatt, R. J. *Inorg. Chem.* **2005**, *44*, 1125. (d) Dinolfo, P. H.; Lee, S. J.; Coropceanu, V.; Bredas, J.-L.; Hupp, J. T. *Inorg. Chem.* **2005**, *44*, 5789. (e) Nohra, B.; Graule, S.; Lescop, C.; Reau, R. *J. Am. Chem. Soc.* **2006**, *128*, 3520. (f) Newkome, G. R.; Wang, P.; Moorefield, C. N.; Cho, T. J.; Mohapatra, P. P.; Li, S.; Hwang, S.-H.; Lukoyanova, O.; Echegoyen, L.; Palagallo, J. A.; Iancu, V.; Hla, S.-W. *Science* **2006**, *312*, 1782. (g) Lee, S. J.; Lin, W. *Acc. Chem. Res.* **2008**, *41*, 521. (h) Zangrado, E.; Casanova, M.; Alessio, E. *Chem. Rev.* **2008**, *108*, 4979. (i) Wang, J.-L.; Li, X.; Lu, X.; Hsieh, I.-F.; Cao, Y.; Moorefield, C. N.; Wesdemiotis, C.; Cheng, S. Z. D.; Newkome, G. R. *J. Am. Chem. Soc.* **2011**, *133*, 11450. (j) Thanasekaran, P.; Lee, C.; Lu, K.-L. *Acc. Chem. Res.* **2012**, *45*, 1403. (k) Wiester, M. J.; Mirkin, C. A. *Inorg. Chem.* **2009**, *48*, 8054. (l) Mondal, A.; Li, Y.; Seuleiman, M.; Julve, M.; Toupet, L.; Buron-Le Cointe, M.; Lescouezec, R. *J. Am. Chem. Soc.* **2013**, *135*, 1653.

(2) (a) Kuehl, C. J.; Yamamoto, T.; Seidel, S. R.; Stang, P. J. *Org. Lett.* **2002**, *4*, 913. (b) Saalfrank, R. W.; Glaser, H.; Demleitner, B.; Hampel,

F.; Chowdhry, M. M.; Schünemann, V.; Trautwein, A. X.; Vaughan, G. B. M.; Yeh, R.; Davis, A. V.; Raymond, K. N. *Chem.—Eur. J.* **2002**, *8*, 493. (c) Kumazawa, K.; Biradha, K.; Kusukawa, T.; Okano, T.; Fujita, M. *Angew. Chem., Int. Ed.* **2003**, *42*, 3909. (d) Pluth, M. D.; Bergman, R. G.; Raymond, K. N. *J. Am. Chem. Soc.* **2008**, *130*, 6362. (e) Lusby, P. J.; Müller, P.; Pike, S. J.; Slawin, A. M. Z. *J. Am. Chem. Soc.* **2009**, *131*, 16398. (f) Pluth, M. D.; Fiedler, D.; Mugridge, J. S.; Bergman, R. G.; Raymond, K. N. *Proc. Natl. Acad. Sci. U.S.A.* **2009**, *106*, 10438. (g) Yoshizawa, M.; Klosterman, J. K.; Fujita, M. *Angew. Chem., Int. Ed.* **2009**, *48*, 3418. (h) Sun, Q.-F.; Iwasa, J.; Ogawa, D.; Ishido, Y.; Sato, S.; Ozeki, T.; Sei, Y.; Yamaguchi, K.; Fujita, M. *Science* **2010**, *328*, 1144. (i) Wang, M.; Zheng, Y.-R.; Ghosh, K.; Stang, P. J. *J. Am. Chem. Soc.* **2010**, *132*, 6282. (j) Wang, M.; Zheng, Y.-R.; Cook, T. R.; Stang, P. J. *Inorg. Chem.* **2011**, *50*, 6107. (k) Paul, L. E. H.; Therrien, B.; Furrer, J. *Inorg. Chem.* **2012**, *51*, 1057.

(3) (a) Barboiu, M.; Vaughan, G.; Graff, R.; Lehn, J.-M. *J. Am. Chem. Soc.* **2003**, *125*, 10257. (b) Giuseppone, N.; Schmitt, J.-L.; Lehn, J.-M. *J. Am. Chem. Soc.* **2006**, *128*, 16748. (c) Heo, J.; Jeon, Y.-M.; Mirkin, C. A. *J. Am. Chem. Soc.* **2007**, *129*, 7712. (d) Hiraoka, S.; Sakata, Y.; Shionoya, M. *J. Am. Chem. Soc.* **2008**, *130*, 10058. (e) Dalgarno, S. J.; Power, N. P.; Atwood, J. L. *Coord. Chem. Rev.* **2008**, *252*, 825. (f) Ward, M. D. *Chem. Commun.* **2009**, 4487. (g) Mirtschin, S.; Slabon-Turski, A.; Scopelliti, R.; Velders, A. H.; Severin, K. *J. Am. Chem. Soc.* **2010**, *132*, 14004. (h) Meng, W.; Breiner, B.; Rissanen, K.; Thoburn, J. D.; Clegg, J. K.; Nitschke, J. R. *Angew. Chem., Int. Ed.* **2011**, *50*, 3479.

(4) (a) Söntjens, S. M. H.; Sijbesma, R. P.; van Genderen, M. H. P.; Meijer, E. W. *J. Am. Chem. Soc.* **2000**, *122*, 7487. (b) Schmuck, C.; Wienand, W. *Angew. Chem., Int. Ed.* **2001**, *40*, 4363. (c) Berl, V.; Schmutz, M.; Krische, M. J.; Khoury, R. G.; Lehn, J.-M. *Chem.—Eur. J.* **2002**, *8*, 1227. (d) Hofmeier, H.; Hoogenboom, R.; Wouters, M. E. L.; Schubert, U. S. *J. Am. Chem. Soc.* **2005**, *127*, 2913.

(5) (a) Brunsveld, L.; Folmer, B. J. B.; Meijer, E. W.; Sijbesma, R. P. *Chem. Rev.* **2001**, *101*, 4071. (b) Lehn, J.-M. *Prog. Polym. Sci.* **2005**, *30*, 814. (c) De Greef, T. F. A.; Meijer, E. W. *Nature* **2008**, *453*, 171. (d) Jiang, W.; Winkler, H. D. F.; Schalley, C. A. *J. Am. Chem. Soc.* **2008**, *130*, 13852. (e) De Greef, T. F. A.; Smulders, M. M. J.; Wolffs, M.; Schenning, A. P. H. J.; Sijbesma, R. P.; Meijer, E. W. *Chem. Rev.* **2009**, *109*, 5687. (f) Jiang, W.; Schalley, C. A. *Proc. Natl. Acad. Sci. U.S.A.* **2009**, *106*, 10425. (g) Jiang, W.; Sattler, D.; Rissanen, K.; Schalley, C. A. *Org. Lett.* **2011**, *13*, 4502. (h) Jiang, W.; Nowosinski, K.; Löw, N. L.; Dzyuba, E. V.; Klautzsch, F.; Schäfer, A.; Huuskonen, J.; Rissanen, K.; Schalley, C. A. *J. Am. Chem. Soc.* **2012**, *134*, 1860.

(6) (a) Wheaton, C. A.; Jennings, M. C.; Puddephatt, R. J. *J. Am. Chem. Soc.* **2006**, *128*, 15370. (b) Chow, C.-F.; Fujii, S.; Lehn, J.-M. *Angew. Chem., Int. Ed.* **2007**, *46*, 5007. (c) Friese, V. A.; Kurth, D. G. *Coord. Chem. Rev.* **2008**, *252*, 199. (d) Parimal, K.; Witlicki, E. H.; Flood, A. H. *Angew. Chem., Int. Ed.* **2010**, *49*, 4628. (e) Chakrabarty, R.; Mukherjee, P. S.; Stang, P. J. *Chem. Rev.* **2011**, *111*, 6810 (and references therein).

(7) Zheng, Y.-R.; Zhao, Z.; Wang, M.; Ghosh, K.; Pollock, J. B.; Cook, T. R.; Stang, P. J. *J. Am. Chem. Soc.* **2010**, *132*, 16873.

(8) Saha, M. L.; Pramanik, S.; Schmittel, M. *Chem. Commun.* **2012**, *48*, 9459.

(9) (a) Sun, S.-S.; Anspach, J. A.; Lees, A. J. *Inorg. Chem.* **2002**, *41*, 1862. (b) Sun, S.-S.; Stern, C. L.; Nguyen, S. T.; Hupp, J. T. *J. Am. Chem. Soc.* **2004**, *126*, 6314. (c) Harano, K.; Hiraoka, S.; Shionoya, M. *J. Am. Chem. Soc.* **2007**, *129*, 5300. (d) Mal, P.; Schultz, D.; Beyeh, K.; Rissanen, K.; Nitschke, J. R. *Angew. Chem., Int. Ed.* **2008**, *47*, 8297. (e) Zhao, L.; Northrop, B. H.; Stang, P. J. *J. Am. Chem. Soc.* **2008**, *130*, 11886. (f) Granzhan, A.; Riis-Johannessen, T.; Scopelliti, R.; Severin, K. *Angew. Chem., Int. Ed.* **2010**, *49*, 5515. (g) Campbell, V. E.; de Hatten, X.; Delsuc, N.; Kauffmann, B.; Huc, I.; Nitschke, J. R. *Nat. Chem.* **2010**, *2*, 684. (h) Fan, J.; Saha, M. L.; Song, B.; Schönherr, H.; Schmittel, M. *J. Am. Chem. Soc.* **2012**, *134*, 150.

(10) (a) Schmittel, M.; Ganz, A. *Chem. Commun.* **1997**, 999. (b) Schmittel, M.; Lüning, U.; Meder, M.; Ganz, A.; Michel, C.; Herderich, M. *Heterocycl. Commun.* **1997**, *3*, 493. (c) Schmittel, M.; Ganz, A.; Fenske, D. *Org. Lett.* **2002**, *4*, 2289. (d) Schmittel, M.; Ammon, H.; Kalsani, V.; Wiegrefe, A.; Michel, C. *Chem. Commun.* **2002**, 2566. (e) Schmittel, M.; Kalsani, V.; Fenske, D.; Wiegrefe, A. *Chem. Commun.* **2004**, 490. (f) Schmittel, M.; Kishore, R. S. K. *Org. Lett.* **2004**, *6*, 1923. (g) Schmittel, M.; Kalsani, V.; Bats, J. W. *Inorg. Chem.* **2005**, *44*, 4115. (h) Schmittel, M.; Kalsani, V.; Michel, C.; Mal, P.; Ammon, H.; Jäckel, F.; Rabe, J. P. *Chem.—Eur. J.* **2007**, *13*, 6223. (i) Fan, J.; Bats, J. W.; Schmittel, M. *Inorg. Chem.* **2009**, *48*, 6338. (j) Schmittel, M.; Mahata, K. *Chem. Commun.* **2010**, *46*, 4163.

(11) (a) Schmittel, M.; Kalsani, V.; Kishore, R. S. K.; Cölfen, H.; Bats, J. W. *J. Am. Chem. Soc.* **2005**, *127*, 11545. (b) Schmittel, M.; He, B.; Mal, P. *Org. Lett.* **2008**, *10*, 2513. (c) Schmittel, M.; Mal, P. *Chem. Commun.* **2008**, 960. (d) Mahata, K.; Schmittel, M. *J. Am. Chem. Soc.* **2009**, *131*, 16544. (e) Schmittel, M.; Samanta, S. K. *J. Org. Chem.* **2010**, *75*, 5911.

(12) (a) Schmittel, M.; He, B.; Fan, J.; Bats, J. W.; Engeser, M.; Schlosser, M.; Deiseroth, H. J. *Inorg. Chem.* **2009**, *48*, 8192. (b) Samanta, S. K.; Samanta, D.; Bats, J. W.; Schmittel, M. *J. Org. Chem.* **2011**, *76*, 7466. (c) Neogi, S.; Schnakenburg, G.; Lorenz, Y.; Engeser, M.; Schmittel, M. *Inorg. Chem.* **2012**, *51*, 10832.

(13) (a) Chou, C.-C.; Liu, H.-J.; Chao, L. H.-C. *Chem. Commun.* **2009**, 6382. (b) Dry, E. F. V.; Clegg, J. K.; Breiner, B.; Whitaker, D. E.; Stefak, R.; Nitschke, J. R. *Chem. Commun.* **2011**, *47*, 6021. (c) Fang, Y.; Murase, T.; Sato, S.; Fujita, M. *J. Am. Chem. Soc.* **2013**, *135*, 613.

(14) (a) Schmittel, M.; He, B. *Chem. Commun.* **2008**, 4723. (b) Schmittel, M.; Michel, C.; Liu, S.-X.; Schildbach, D.; Fenske, D. *Eur. J. Inorg. Chem.* **2001**, 1155. (c) Ogi, S.; Ikeda, T.; Wakabayashi, R.; Shinkai, S.; Takeuchi, M. *Chem.—Eur. J.* **2010**, *16*, 8285.

(15) Schmittel, M.; Michel, C.; Wiegrefe, A.; Kalsani, V. *Synthesis* **2001**, 1561.

(16) (a) Engeser, M.; Rang, A.; Ferrer, M.; Gutierrez, A.; Baytekin, H. T.; Schalley, C. A. *Int. J. Mass Spectrom.* **2006**, *255/256*, 185. (b) Ferrer, M.; Gutiérrez, A.; Mounir, M.; Rossell, O.; Ruiz, E.; Rang, A.; Engeser, M. *Inorg. Chem.* **2007**, *46*, 3395. (c) Rang, A.; Engeser, M.; Maier, N. M.; Nieger, M.; Lindner, W.; Schalley, C. A. *Chem.—Eur. J.* **2008**, *14*, 3855. (d) Baytekin, H. T.; Sahre, M.; Engeser, M.; Rang, A.; Schulz, A.; Schalley, C. A. *Small* **2008**, *4*, 1823. (e) Rodríguez, L.; Lima, J. C.; Ferrer, M.; Rossell, O.; Engeser, M. *Inorg. Chim. Acta* **2012**, *381*, 195. (f) Ferrer, M.; Gutiérrez, A.; Rodríguez, L.; Rossell, O.; Ruiz, E.; Engeser, M.; Lorenz, Y.; Schilling, R.; Gómez-Sahl, P.; Martín, A. *Organometallics* **2012**, *31*, 1533.

(17) Delpuech, J.-J., Ed.; *Dynamics of Solutions and Fluid Mixtures by NMR*; John Wiley and Sons Ltd.: New York, 1995.

(18) (a) Megyes, T.; Jude, H.; Grósz, T.; Bakó, I.; Radnai, T.; Tárkányi, G.; Pálinkás, G.; Stang, P. J. *J. Am. Chem. Soc.* **2005**, *127*, 10731. (b) Ghosh, K.; Hu, , J.; White, H. S.; Stang, P. J. *J. Am. Chem. Soc.* **2009**, *131*, 6695. (c) Chan, Y.-T.; Li, X.; Yu, J.; Carri, G. A.; Moorefield, C. N.; Newkome, G. R.; Wesdemiotis, C. *J. Am. Chem. Soc.* **2011**, *133*, 11967.

(19) Frisch, M. J. et al. *Gaussian 03*; Gaussian, Inc.: Wallingford, CT, 2004.

(20) Becke, A. D. *J. Chem. Phys.* **1993**, *98*, 5648.

(21) Hay, P. J.; Wadt, W. R. *J. Chem. Phys.* **1985**, *82*, 299.

(22) (a) Fujita, M.; Kwon, Y. J.; Washizu, S.; Ogura, K. *J. Am. Chem. Soc.* **1994**, *116*, 1151. (b) Blake, A. J.; Hill, S. J.; Hubberstey, P.; Li, W. S. *J. Chem. Soc., Dalton Trans.* **1997**, 913. (c) Noguchi, D.; Tanaka, H.; Kondo, A.; Kajiro, H.; Noguchi, H.; Ohba, T.; Kanoh, H.; Kaneko, K. *J. Am. Chem. Soc.* **2008**, *130*, 6367.